

**Universitat de Lleida**

Document downloaded from:

<http://hdl.handle.net/10459.1/72111>

The final publication is available at:

<https://doi.org/10.1007/s11357-020-00210-3>

Copyright

(c) Springer, 2020

# Gene expression and regulatory factors of the mechanistic target of rapamycin (mTOR) complex 1 predict mammalian longevity

Natalia Mota-Martorell<sup>1</sup>, Mariona Jove<sup>1</sup>, Irene Pradas<sup>1</sup>, Rebeca Berdún<sup>1</sup>, Isabel Sanchez<sup>2</sup>, Alba Naudi<sup>1</sup>, Eloi Gari<sup>3</sup>, Gustavo Barja<sup>4,\*</sup>, Reinald Pamplona<sup>1,\*</sup>

<sup>1</sup>Department of Experimental Medicine, University of Lleida-Lleida Biomedical Research Institute (UdL-IRBLleida), Lleida, Catalonia, Spain

<sup>2</sup>Genomics Unit, Lleida Biomedical Research Institute (IRBLleida), Lleida, Catalonia, Spain

<sup>3</sup>Department of Basic Medical Sciences, University of Lleida-Institute of Research in Biomedicine of Lleida (UdL-IRBLleida), Lleida, Catalonia, Spain

<sup>4</sup>Department of Genetics, Physiology and Microbiology, Complutense University of Madrid, Madrid, Spain

\* Corresponding authors:

Dr. Gustavo Barja; e-mail: [gbarja@bio.ucm.es](mailto:gbarja@bio.ucm.es);

Dr. Reinald Pamplona; e-mail: [reinald.pamplona@mex.udl.cat](mailto:reinald.pamplona@mex.udl.cat)

Short title: mTORC1 and longevity

## Abstract

Maximum longevity (ML) varies significantly across animal species, but the underlying molecular mechanisms remain poorly understood. Recent studies and omics approaches suggest that phenotypic traits of ML could converge in the mammalian target of rapamycin (mTOR) signalling pathway. The present study is a comparative approach using heart tissue from 8 mammalian species with a ML ranging from 3.5 to 46 years. Gene expression, protein content, and concentration of regulatory metabolites of the mTOR complex 1 (mTORC1) were measured using droplet digital PCR, western blot and mass spectrometry, respectively. Our results demonstrate 1) the existence of differences species-specific in gene expression and protein content of mTORC1; 2) that the achievement of a longevity phenotype requires decreased and inhibited mTORC1; 3) decreased content of mTORC1 activators in long-lived animals, and 4) independence of phylogeny relationships on these changes. Altogether, our findings support mTORC1 down-regulation to achieve a longevous phenotype.

### *Key words:*

Arginine, droplet digital PCR, FKBP12, leucine, longevity, mass spectrometry, metabolomics, methionine cycle metabolites, mTOR, phylogeny, PRAS40, raptor, western blot

## Introduction

Maximum longevity (ML) is a species-specific trait that differ more than 5000-fold among animal species, and more than 100-fold among mammals (Ma and Gladyshev 2017). The ML of animal species is an optimised intrinsic feature genetically determined and regulated and accomplished by slowing the rate of aging (Jones et al. 2014). As during evolution speciation has demanded specific mutations directed to favour species adaptations (Ma et al. 2015), the molecular substrates determining ML are thought to be also conserved.

The discovery of the molecular bases of mammalian ML usually take advantage of the use of long-lived animal models (Barja 1998; Perez-Campo et al. 1998; Pamplona et al. 2002; Selman et al. 2009; Wu et al. 2013; Fushan et al. 2015; Ma and Gladyshev 2017; Sahm et al. 2018), the performance of comparative studies across animal species differing in ML (Barja 1998; Perez-Campo et al. 1998; Pamplona et al. 2002; Jové et al. 2013; Naudí et al. 2013; Ma et al. 2015; Ma et al. 2016; Bozek et al. 2017; Mota-Martorell et al. 2019), and the induction of genetic manipulations as well as pharmacological and nutritional interventions designed to achieve a longevity extension (Pamplona and Barja 2006; Pamplona and Barja 2011; Longo et al. 2015)

Among the phenotypic features associated with long-lived animal species can be mentioned lower generation of endogenous damage, highly resistant macromolecular components concerning nucleotides, proteins and lipids, and specific transcriptomics and metabolomics profiles, among others (Pamplona and Barja 2007; Pamplona and Barja 2011; Naudí et al. 2013; Ma and Gladyshev 2017; Lewis et al. 2018; Tyshkovskiy et al. 2019). Notably, several of these features seem to converge to and could be supported by specific cell signalling pathways and, in particular, by the mechanistic target of rapamycin (mTOR) pathway.

mTOR, member of an evolutionary conserved group of serine/threonine kinases from the PIKK (phosphatidylinositol-3 kinases (PI3K)-related kinase) family, is present as two distinct complexes: mTOR complex 1 (mTORC1) and mTOR complex 2 (mTORC2) (Valvezan and Manning 2019). mTORC1 is sensitive to rapamycin and plays a central role in the mTOR signalling network monitoring and integrating a broad diversity of extra- and intracellular signals and controlling cell physiology. Thus, mTORC1 through a wide range of downstream pathways such as mRNA translation, biosynthesis pathways, mitochondrial function, autophagy, endoplasmic reticulum stress, and stress responses, among others, can regulate cell metabolism, growth, and proliferation, and to modulate complex physiological processes such as aging and longevity (Kapahi et al. 2010; Antikainen et al. 2017; Weichhart 2018; Papadopoli et al. 2019; Valvezan and Manning 2019). In this line, inhibition of the mTOR pathway results in longevity extension in several animal models (from yeast to mice) (Kapahi et al. 2010; Lushchak et al. 2017; Weichhart 2018; Papadopoli et al. 2019); whereas activation of mTOR pathway results in longevity shortening derived from the aging process itself and the generation of pathological conditions such as cancer, diabetes, and neurodegenerative diseases (Kapahi et al. 2010; Johnson et al. 2013; Papadopoli et al. 2019).

In mammals, mTORC1 is composed by mTOR and its associated proteins Raptor (regulatory associated protein of TOR), mLst8 (mammalian lethal with SEC13 protein 8), PRAS40 (Proline-rich AKT1 substrate of 40 kDa), and Deptor (DEP domain-containing mTOR-interacting protein) (Valvezan and Manning 2019). Importantly, Raptor and PRAS40 are present exclusively in

mTORC1. Whereas mTOR, Raptor, and mLST8 are core components, DEPTOR and PRAS40 are inhibitory subunits. In addition, FK506 binding protein (FKBP12) is a regulatory subunit of the mTORC1 activity and sensitive to rapamycin. Among extra- and intracellular signals that regulate mTORC1 activity can be mentioned growth factors, hormones, glucose, ATP, oxygen, metabolic intermediates, and amino acids (Valvezan and Manning 2019). Among amino acids, arginine, leucine, and methionine cycle metabolites play a relevant role as activators of mTORC1 through their interaction with several and diverse intracellular mediators (Valvezan and Manning 2019).

Despite the evolutionary conservation of the mTORC1, we unknown if differences exist among mammalian species, and if they are related to longevity. In order to examine the molecular traits associated with the mammalian longevity we used droplet digital PCR (ddPCR) and western blot methods to define the steady-state levels of gene expression and protein content of the mTORC1, and targeted metabolomics to measure the concentration of its activators. Heart tissue of eight mammalian species showing more than one order of magnitude of difference in ML —from 3.5 years in mice to 46 years in horses, was analysed. The selected subunits were: i) mTOR, Raptor, and PRAS40 as exclusive components of the mTORC1; ii) FKBP12 as regulatory subunit of the mTORC1 activity; and iii) arginine, leucine, methionine and its related metabolites as activators of the mTORC1 activity. We have found a specific modulation of the mTORC1 in long-lived animals that might contribute to an extended longevity phenotype.

## Results

In order to determine whether heart mTORC1 gene expression and protein content differed among mammals, multivariate statistics were applied. Non-supervised principal component analysis (PCA) revealed the existence of a species-specific protein and gene profile of the mTORC1 (Figure 1A), capable to explain up to 61.8% of sample variability. A hierarchical clustering of the samples represented by a heat map revealed specific mTORC1 patterns for rodents (mouse, rat, gerbil and guinea pig) (Figure 1B). Furthermore, this global pattern found in rodents was different from that found in non-rodents (rabbit, pig, cow and horse) (Figure 1C). These results were confirmed by performing a supervised analysis, such as partial least squares discriminant analysis (PLS-DA) (Figure 1D). Cross-validation values of PLS-DA model (Figure 1E) showed that heart gene expression and protein amount of mTORC1 is a good model to define the animal species obtaining an accuracy value and  $R^2$  of 0.6 using only 5 components. The discriminating power between groups of the different measured features was ranked by applying a variable importance projection (VIP) score (Figure 1F). After selecting those features with VIP score > 1.5 as significant, the *mtor* gene expression and FKBP12 protein content were found to be the top-ranked features.

The gene expression and protein content of mTORC1 were also correlated with animal ML (Figure 2). Specifically, long-lived animals have increased *mtor* expression, but decreased *raptor* (Figure 2A). Lesser protein content of mTOR and Raptor was also found in long-lived animals, but increased PRAS40 (Figure 2B). Furthermore, gene and protein content of Raptor was positively correlated (Supplementary figure 1). Regarding protein phosphorylation, increased mTOR<sup>Ser2448</sup> and decreased PRAS40<sup>Thr246</sup> was found in long-lived animals (Figure 2B). Interestingly, the protein content of mTOR and PRAS40 is inversely correlated with their degree of phosphorylation (Supplementary figure 1).

Because the relevance of regulatory factors such as FKBP12, as well as specific metabolites like arginine, leucine and methionine cycle metabolites in determining mTORC1 activity, we have analysed the gene expression and protein content of FKBP12, as well as the content of the different metabolites using mass spectrometry and evaluated their relationship with ML and mTORC1 core components (Figure 3). Thus, two well-known positive activators of mTOR, arginine and methionine, as well as two methionine-related metabolites, such as SAM and homocysteine, were found to be negatively correlated with animal ML (Figure 4A, B). Gene expression of *fkbp1a* and protein content of FKBP12 were also negatively correlated with animal ML (Figure 4C). Therefore, the greater the ML of a mammalian species, the lower is its tissue concentration of regulatory metabolites of mTORC1. In addition, methionine metabolites were associated with mTOR, PRAS40 and Raptor (Figure 3). Accordingly, methionine and SAM were positively associated to Raptor and PRAS40<sup>Thr246</sup>, but negatively to PRAS40<sup>Thr246</sup>; SAM was also negatively correlated with mTOR<sup>Ser2448</sup>; whereas that homocysteine was only positively correlated with PRAS40<sup>Thr246</sup> (Figure 5). Arginine was positively correlated with PRAS40<sup>Thr246</sup> and FKBP12, but negatively with PRAS40 (Figure 6A). Finally, the regulatory factor FKBP12 showed a positive correlation with mTOR and RAPTOR, whereas the correlation was negative for phosphorylated mTOR (Figure 6B).

Animal species are evolutionary related, raising the possibility that data from closely related species may be not necessarily statistically independent from one another. Therefore, to correct for phylogeny we performed a phylogenetically generalised least squares regression (PGLS) following the phylogenetic tree constructed in [Figure 6A](#). First of all, we have measured the amount of phylogenetic signal of each trait (Pagel's  $\lambda$ ). Basically, it indicates the degree up to which a specific trait is influenced by phylogeny, indicating whether the changes in those traits across different species might be due to phylogenetic relationships ( $\lambda=1$ ) or not ( $\lambda=0$ ). After correcting for phylogenetic relationships, the expression of *mtor* ( $p=0.032$ ,  $R^2=0.1$ ), *rptor* ( $p<0.001$ ,  $R^2=0.4$ ) and *fkbp1a* ( $p=0.001$ ,  $R^2=0.3$ ), mTOR<sup>Ser2448</sup> ( $p=0.05$ ,  $R^2=0.48$ ) PRAS40<sup>Thr246</sup> ( $p=0.038$ ,  $R^2=0.5$ ) and methionine ( $p=0.003$ ,  $R^2=0.83$ ) remained to be correlated with mammalian longevity ([Figure 6B](#)). Among them, mTOR<sup>Ser2448</sup> and PRAS40<sup>Thr246</sup> appeared to individually explain 48% of the animal ML variability.

## Discussion

### Longevity-associated mTORC1 profile

We have found that animal species have a unique species-specific mTORC1 profile, which is associated to animal longevity. Furthermore, our model revealed that mTORC1 accounts for 60% of inter-species variation, being gene expression and protein phosphorylation the highest longevity predictors. In agreement, previous studies had already described a unique gene expression profile (Caron et al. 2015; Fushan et al. 2015; Ma et al. 2016; Muntané et al. 2018), metabolome (Ma et al. 2015) and lipidome (Jové et al. 2013; Mota-Martorell et al. 2019) for long-lived species. Since mTORC1 is known to be a master regulator of the cellular metabolism, modulating both mRNA translation and lipid metabolism (Caron et al. 2015), these findings support the idea of the existence of important genetic adaptations in nutrient-sensing metabolic pathways, such as mTOR, in the evolution of longevity (Singh et al. 2019).

### Decreased mTORC1 content and activity to achieve a longevity phenotype

The longevity phenotype is achieved by decreasing mTORC1 content and activity. Genetically, long-lived animals have decreased *rptor* but increased *mtor*. Accordingly, it has been reported that nonagenarians' blood has decreased mRNA content of *mtor*, *akt1s1* and *rptor* when compared with middle-aged controls (Passtoors et al. 2013). Moreover, the offspring of those long-lived individuals had also decreased *rptor* gene expression, arising as a potential biomarker of familiar longevity. Protein content of mTOR and Raptor were also decreased in long-lived animals, supporting the role of Raptor in longevity.

mTORC1 is regulated by opposite phosphorylation patterns in mTOR and PRAS40. mTOR phosphorylation at serine 2448 has been found to have inhibitory effects in skeletal muscle (Figueiredo et al. 2017). Nutrient availability promotes mTOR activation which, in turn, activates p70S6K that re-phosphorylates mTOR (at Ser<sup>2448</sup>) to inhibit its activity. The existence of this negative loop explains why in some studies increased Ser2448 is found in starving conditions (Chiang and Abraham 2005). However, PRAS40 phosphorylation at Thr<sup>246</sup> via Akt results on its dissociation from mTORC1, which is then released and active (Nascimento et al. 2010). Accordingly, we have found increased mTOR<sup>Ser2448</sup> and PRAS40, but decreased PRAS40<sup>Thr246</sup> in long-lived animals, suggesting that inhibition of the mTORC1 is needed to achieve a longevity phenotype. Previous studies had already reported inhibitory changes of mTORC1 activators (Ma and Gladyshev 2017) in whales (estimated longevity above 200 years). Genetic mutations in mTOR (Wu et al. 2013) or its downstream effector S6K1 (Selman et al. 2009) increases lifespan in mice, as well as its pharmacological inhibition with rapamycin (Singh et al. 2019).

Achievement of longevity is not only due to changes on the mTORC1 itself, but to its activity regulators. Although it might sound controversial, decreased gene expression and protein content of the inhibitor FKBP12 was found in long-lived animals. However, since mTORC1 total content is decreased, less inhibitors are needed, allowing to save the energy that otherwise will be used to synthesize protein. Besides, recent studies have revealed that FKBP12 is associated with neurotoxicity (Caraveo et al. 2017), but its disruption enhances mTOR-Raptor interactions and memory (Hoeffler et al. 2008). Therefore, these results suggest that

maintenance of proper mTORC1 stability by decreasing FKBP12 might be a molecular trait of animal longevity.

Decreased concentration of mTORC1 activators, such as arginine and methionine-related metabolites, might enhance its down-regulation. Accordingly, arginine content in primate fibroblasts has been shown to be negatively correlated with longevity (Ma et al. 2016). Besides, lower plasma methionine had already been described in the naked-mole rat (Lewis et al. 2018), as well as increased methionine, SAM and homocysteine in ageing mice liver (Jeon et al. 2018).

### **mTORC1 and methionine-metabolism: the longevity connexion**

mTORC1 is often described as a master regulator of cellular metabolism, being responsible of modulating anabolic and catabolic processes, such as protein turnover. Therefore, a number of authors proposed that mTORC1 inhibition during dietary restriction promotes autophagy, which clears old and dysfunctional organelle, promoting a lifespan extension (Simonsen et al. 2008). Supporting this idea, methionine restriction has been found to require autophagy to mediate its life span extension effects (Ruckenstuhl et al. 2014; Bárcena et al. 2019). Furthermore, a study in worms suggested that SAMTOR detects methionine availability via SAM (Gu et al. 2017). Overall, these results support that autophagy induction via mTORC1 down-regulation or inhibition might be a key mechanism to promote lifespan.

In our model, we have been able to establish a correlation between the mTORC1-longevity associated changes and the methionine metabolism. Specifically, we have found that methionine, homocysteine and arginine might influence PRAS40 phosphorylation, whereas SAM might influence mTOR phosphorylation. Furthermore, methionine and SAM change with Raptor, supporting the idea that it might be a key factor modulating animal longevity. However, more studies need to be done to confirm these new insights regarding mTORC1 modulation in animal longevity (Figure7). mTORC1 activity has also been related to increased mitochondrial activity (Schieke et al. 2006; Cunningham et al. 2007), as well as increased *de novo* lipid biosynthesis and protein synthesis (Düvel et al. 2010), that might favour the long-lived phenotype.

### **Assessing inter-species issues**

Comparative studies across species with different lifespan are a powerful source of information to identify mechanisms linked to extended longevity (Ma et al. 2015; Ma et al. 2016; Bozek et al. 2017). However, those kinds of studies come up with several problems that need to be faced. First, the evolutionary relationships doesn't allow for independence of the data (Cooper et al. 2016). Therefore, we don't know if a specific trait correlates to longevity differences, or alternatively, whether these differences arise because the similarity of the data. To overcome this limitation, we have carried out statistical analyses accounting for these phylogenetic relationships. In this way, we've found that phylogeny has greater influence on protein content and activity compared to gene expression, suggesting that gene content is an intrinsic property of long-lived animals.

The second problem that needs to be assessed is technical, due to the presence of SNPs inducing amino acid variations. Although the mTOR pathway is highly conserved across living organisms (Fontana et al. 2010), the small variations in protein structure could decrease antibody recognition. To overcome these methodological issues, we used degenerated primers capable to recognise sequences with SNPs. Globally, the protein data was supported by the gene analyses. However, the correlation of the mTOR gene and protein content still followed opposite trends. Cellular abundance of proteins have been demonstrated to be predominantly controlled at the level of translation (Schwanhäusser et al. 2011). Therefore, those differences might be due to technical issues or by different translation regulation.

## **Conclusions**

Altogether, the obtained results support the given role of the mTORC1 in regulating mammalian longevity. Specially, we've provided insight of the influence of gene expression, total protein content as well as the importance of modulating the basal levels of mTORC1 activation. Indeed, we suggest that maintaining decreased and inhibited mTORC1 is essential to achieve a long-lived phenotype. Thereby, the mechanisms that regulate mTOR activity might prompt new insights regarding mammalian longevity.

## Material and Methods

### Animals

Mammalian species included in the study were male adult specimens with an age representing their 15-30% of their ML. The recorded values for ML (in years) were: mouse (*Mus musculus*), 3.5; rat (*Rattus norvegicus*), 4.5; gerbil (*Meriones unguiculatus*), 6.3 guinea pig (*Cavia porcellus*), 8; rabbit (*Oryctolagus cuniculus*), 13; pig (*Sus scrofa*), 27; cow (*Bos taurus*), 30; and horse (*Equus caballus*), 46. Rodents and rabbits were obtained from rodent husbandries and sacrificed by decapitation, whereas sheep, pigs, cow and horses were obtained from abattoirs. The animal care protocols were approved by the Animal Experimentation Ethics committee of the University of Lleida. Heart ventricles from 5-7 animals were removed and immediately frozen in liquid nitrogen and transferred to -80°C until analyses.

### Protein content determination

Protein content was measured performing Western Blot analyses as previously described (Martínez-Cisuelo et al. 2016). Immunodetection was performed using antibodies against mTOR (2972, Cell signalling), mTOR<sup>Ser2448</sup> (2971, Cell signalling), PRAS40 (ab151718, Abcam), PRAS40<sup>Thr246</sup> (ab134084, Abcam), RAPTOR (ab189158) and FKBP12 (ab2981, Abcam). Secondary antibodies were anti-mouse (NA931 GE, Healthcare) and anti-rabbit (31460, Pierce). Densitometry values were referred to total protein content (for phosphorylated proteins) and its respective coomassie staining (Supplementary figure 2).

### Gene expression

Heart RNA was extracted using RNeasy Fibrous Tissue Mini Kit (Qiagen, Germany) and retro-transcribed to cDNA using the High-Capacity cDNA Reverse Transcription kit (Applied Biosystems, USA). Degenerate primers were designed to amplify conserved regions among mammalian sequences and using the software PriFi (Fredslund et al. 2005). DNA amplification was performed by droplet digital PCR (ddPCR) on the basis of EvaGreen ddPCR Supermix (BioRad, Barcelona). The results from more than 12.000 droplets were accepted and normalised to an appropriate housekeeping (*ndufa9*). Values are reported as cDNA gene units per cDNA housekeeping units. All equipment and reagents were purchased from Bio-Rad (Barcelona, Spain).

### Targeted metabolomics

#### Sample processing

Plasma metabolites extraction was performed based on the methodology previously described (Method 1, Cabré et al. 2016). Briefly, 10 µL of plasma were added to 30 µL of cold methanol containing 1 µg/mL of Phe-<sup>13</sup>C as internal standard and 1 µM butylhydroxytoluene as antioxidant. Then, samples were incubated at room temperature for 15 min and centrifuged at 12000 g for 3 min. Finally, the supernatant was filtrated through a 0.22-µm organic diameter filter (Sigma, CLS8169) and 200 µL were transferred to Agilent vials with glass inserts for further analysis.

Sulphur-containing metabolites were extracted on the bases of the methodology previously described (Method 2, Liu et al. 2017). Briefly, 2 µL of 5% DTT were added to 10 µL of plasma. The resulting solution was vortexed for 1 min and allowed to stand at room temperature for 10 min. For protein precipitation, 40 µL of 0.1% formic acid plus 0.05% trifluoroacetic acid in acetonitrile containing 1 µg/mL of Phe-<sup>13</sup>C as internal standard was added to the sample, and the solution was vortexed for 2 min. Then, samples were incubated at room temperature for 15 min and centrifuged at 12000 g for 3 min. Finally, the supernatant was filtrated through a 0.22-µm organic diameter filter (Sigma, CLS8169) and 200 µL were transferred to Agilent vials with glass inserts for further analysis.

### *Analysis conditions*

The individual conditions for the detection and quantification of heart metabolites are listed in [Table 1](#).

For non-sulphur-containing metabolites, 2 µL of extracted sample was injected based on the method described (Method 1, Cabré et al. 2016). Chromatographic separation was achieved on a reversed-phase column (Zorbax SB-Aq 1.8 µm 2.1×50mm; Agilent Technologies) equipped with a precolumn (Zorba-SB-C8 Rapid Resolution Cartridge 2.1×30mm 3.5 µm; Agilent Technologies) with a column temperature of 60°C. The flow rate was 0.6mL/min during a 19 min. Solvent A was composed of water containing 0.2% acetic acid and solvent B was composed of methanol 0.2% acetic acid. The gradient started at 2% B and increased to 98% B in 13 minutes and held at 98% B for 6 minutes. Post-time was established in 5 minutes. Electrospray ionization was performed in both positive and negative ion mode (depending on the target metabolite) using N<sub>2</sub> at a pressure of 50 psi for the nebulizer with a flow of 12 L/min and a temperature of 325°C, respectively.

For sulphur-containing metabolites, 10 µL of extracted sample was injected based on the method described (Method 2, Liu et al. 2017). Chromatographic separation was achieved on a reversed-phase Supelcosil LC-CN column (Supelco of 4.6 x 250 mm and 5 µL particle size. Sigma) with a column temperature of 30°C. The flow rate was 0.5mL/min during a 10 min at 10%B. Solvent A was composed of water containing 0.1% formic acid and solvent B was composed of acetonitrile 0.1% formic acid. Electrospray ionization was performed in both positive and negative ion mode (depending on the target metabolite) using N<sub>2</sub> at a pressure of 50 psi for the nebulizer with a flow of 12 L/min and a temperature of 325°C, respectively.

Data was collected using the MassHunter Data Analysis Software (Agilent Technologies). Peak determination and peak area integration were carried out with MassHunter Quantitative Analyses (Agilent Technologies. San Jose. CA. USA).

### *Metabolite quantification*

Metabolite quantification was performed by constructing standard curves for each metabolites. Expected plasma concentration for each metabolite was based on the Human Metabolome Database (HMDB, <http://www.hmdb.ca>). Standard curves were constructed by plotting the peak area ratio against the final metabolite concentration.

### Equipment

The analysis was performed through liquid chromatography coupled to a hybrid mass spectrometer with electrospray ionization and a triple quadrupole mass spectrometer. The liquid chromatography system was an ultra-performance liquid chromatography model 1290 coupled to ESI-TQ MQ/MS model 6420 both from Agilent Technologies (Barcelona, Spain).

### Statistics

Multivariate statistics was performed using Metaboanalyst software. Pearson correlation and Pearson partial correlation were performed using IBM SPSS Statistics (v21.0.0). Linear models and phylogenetic generalised least squares regression (PGLS) were constructed using RStudio (v1.1.453). The phylogenetic tree was constructed using taxa names in TimeTree ([www.timetree.org](http://www.timetree.org)). Functions used were included in the package *caper*. Data was log-transformed and mean-centred prior statistical analyses in order to accomplish the assumptions of linearity.

## Acknowledgements

N.M-M Received a predoctoral fellowship from the Generalitat of Catalonia (AGAUR, ref 2018FI\_B2\_00104). We thank Salvador Batolome, from the Laboratory of Luminescence and Biomolecular Spectroscopy (Autonomous University of Barcelona, Barcelona, Catalonia, Spain), for technical support.

## Funding

This work was supported by the Spanish Ministry of Economy and Competitiveness, Institute of Health Carlos III (grant number PI14/00328), the Spanish Ministry of Science, Innovation and Universities (RTI2018-099200-B-I00), and the Generalitat of Catalonia, Agency for Management of University and Research Grants (2017SGR696) and Department of Health (SLT002/16/00250) to R.P. This study has been co-financed by FEDER funds from the European Union (“A way to build Europe”).

## Author Contributions

G.B and R.P designed the study. N.M.M., M.J., I.P., R.B., I.S., A.N., and E.G. performed experimental work. N.M.M and R.P. analysed the data. R.P. supervised the design and data interpretation. The manuscript was written by N.M.M, G.B. and R.P. and edited by R.P. All authors discussed the results and commented on the manuscript.

## Notes

The authors declare no competing financial interest.

## Figure legends

**Figure 1. Multivariate statistics reveals a species-specific gene expression and protein content of mTORC1.** **A)** Principal component analyses (PCA) representation of mTORC1. X: Principal component 1 (PC1); Y: Principal component 2 (PC2); Z: Principal component 3 (PC3). **B)** Hierarchical clustering of individual animal samples according to mTORC1 gene expression and protein content. **C)** Hierarchical clustering of animal species according to average mTORC1 gene expression and protein content. **D)** Partial least squares discriminant analysis (PLS-DA) representation of mTORC1. X: Component 1 (C1); Y: Component 2 (C2); Z: Component 3 (C3). **E)** Cross validation (CV) analyses (10-fold CV method) of the PLS-DA model. **F)** Variable importance projection (VIP) scores indicating the elements which contribute the most to define the first component of a PLS-DA.

**Figure 2. mTORC1 gene expression (A) and protein content and phosphorylation (B) are linearly correlated with mammalian ML.** Pearson correlation was performed between gene expression or protein content and maximum longevity (ML). Linear regression was applied when significant relationships were found.  $R^2(mtor)=0.1$ ;  $R^2(rptor)=0.4$ ;  $R^2(mTOR)<0.1$ ;  $R^2(Raptor)=0.14$ ;  $R^2(PRAS40)=0.22$ ;  $R^2(mTOR^{Ser2448})=0.27$ ;  $R^2(PRAS40^{Thr246})=0.40$ . Minimum significance level was set at  $p<0.05$ . Gene expression and protein content were log-transformed to accomplish the assumptions of normality.

**Figure 3. Pearson correlation matrix of mTORC1 subunits gene expression and protein content and phosphorylation.** Pearson r-value for pairwise comparisons is reported. Non-significant correlations are left in blank. Minimum significance level was set at  $p<0.05$ . Metabolite concentration, gene expression and protein content were log-transformed to accomplish the assumptions of normality.

**Figure 4. Metabolite concentration (A, B), gene expression and protein content (C) of mTORC1 regulators are linearly correlated with mammalian ML.** Pearson correlation was performed between metabolite concentration, gene expression or protein content and maximum longevity (ML). Linear regression was applied when significant relationships were found.  $R^2(\text{Methionine})=0.42$ ;  $R^2(\text{SAM})=0.38$ ;  $R^2(\text{Homocysteine})=0.24$ ;  $R^2(\text{Arginine})=0.16$ ;  $R^2(fkbp1a)=0.33$ ;  $R^2(\text{FKBP12})<0.1$ ; Minimum significance level was set at  $p<0.05$ . Metabolite concentration, gene expression and protein content were log-transformed to accomplish the assumptions of normality.

**Figure 5. Relationships between mTORC1 and methionine-related metabolites in heart tissue from mammalian species.** Pearson correlation was performed. Pearson r values are reported in **Figure 3**. Linear regression (LR) model was performed when significant relationships were found. Minimum significance level was set at  $p<0.05$ . Metabolite concentration, gene expression and protein content were log-transformed to accomplish the assumptions of normality.

**Figure 6. Relationships between the mTORC1 regulators arginine (A) and FKBP12 (B) with mTORC1 components and methionine-related metabolites in heart tissue of mammals.** Pearson correlation was performed. Pearson r values are reported in **Figure 3**. Linear regression (LR) model was performed when significant relationships were found. Minimum

signification level was set at  $p < 0.05$ . Metabolite concentration, gene expression and protein content were log-transformed to accomplish the assumptions of normality.

**Figure 7. mTORC1 is correlated with animal ML after correcting for phylogenetic relationships.** **A)** Phylogeny used and its modification according to Pagel's  $\lambda$ , which is a coefficient that transforms the phylogeny and adopts values between 0-1 when assuming absent ( $\lambda=0$ ) or strong ( $\lambda=1$ ) phylogenetic signal in the data. **B)** Linear regression between the average metabolite concentration, gene expression or protein content and animal ML (black lines) and after correcting for phylogenetic effect (red lines).  $R^2(mtor)=0.1$ ;  $R^2(rptor)=0.4$ ;  $R^2(fkbp1a)=0.27$ ;  $R^2(mTOR^{Ser2448})=0.48$ ;  $R^2(PRAS40^{Thr246})=0.5$ ;  $R^2(\text{Methionine})=0.83$ . Metabolite concentration, gene expression and protein content were log-transformed to accomplish the assumptions of normality.

**Figure 8. Longevity model of the mTORC1 modulation.** Green indicates increased in long-lived animals. Red indicates decreased in long-lived animals.

**Supplementary figure 1. Relationships among the mTORC1 core components in heart tissue from mammalian species.** Pearson correlation was performed. Pearson  $r$  values are reported in **Figure 3**. Linear regression (LR) model was performed when significant relationships were found. Minimum signification level was set at  $p < 0.05$ . Gene expression and protein content were log-transformed to accomplish the assumptions of normality.

**Supplementary figure 2. Individual mTORC1 protein content and phosphorylation from animal's heart.** **A)** mTOR total protein content,  $mTOR^{Ser2448}$  and its respective coomassie. **B)** PRAS40 total protein content,  $PRAS40^{Thr246}$  and its respective coomassie. **C)** RAPTOR protein content and its respective coomassie. **D)** FKBP12 protein content and its respective coomassie.

## Tables

**Table 1.** Analytical traits of the metabolites measured in heart tissue.

Cpd Name	Prec Ion	Prod Ion	Frag (V)	CE (V)	CAV (V)	Ret Time (min)	Ret Window	Polarity	Extraction	Method
<b>AMINO ACIDS</b>										
Arginine	175.1	70.2	60	20	7	0.32	2	Positive	Methanol	1
Arginine	175.1	60.2	60	15	7	0.32	2	Positive	Methanol	1
Cysteine	122.02	76	64	12	7	6.312	4	Positive	DTT	2
Cysteine	122.02	59	64	24	7	6.312	4	Positive	DTT	2
Leucine	132.1	86	64	8	7	0.591	2	Positive	Methanol	1
Leucine	132.1	69	64	16	7	0.591	2	Positive	Methanol	1
<b>METHIONINE METABOLISM</b>										
Homocysteine	136.18	90.1	135	15	7	7.225	4	Positive	DTT	2
Homocysteine	136.18	56.2	135	15	7	7.225	4	Positive	DTT	2
Methionine	150.05	104	64	4	7	0.48	2	Positive	DTT	1
SAM	399.1	250	112	12	7	0.396	2	Positive	DTT	1
SAM	399.1	136	112	28	7	0.396	2	Positive	DTT	1
<b>ISTD</b>										
PheC13	167.09	120.1	70	8	7	0.87	2	Positive	Methanol/DTT	1/2
PheC13	167.09	77	70	44	7	0.87	2	Positive	Methanol/DTT	1/2
PheC13	167.09	103	70	28	7	0.87	2	Positive	Methanol/DTT	1/2
PheC13	167.09	51.1	70	60	7	0.87	2	Positive	Methanol/DTT	1/2

Fragmentor. collision energy (CE) and cell acceleration voltage (CAV) were given as voltage; retention time (RT) in minutes; and product and precursor ion as m/z.

Method 1 (see material and methods, Cabré et al. 2016); Method 2 (see material and methods, Liu et al. 2017).

## References

- Antikainen H, Driscoll M, Haspel G, Dobrowolski R. 2017. TOR-mediated regulation of metabolism in aging. *Aging Cell* 16:1219–1233.
- Bárcena C, López-Otín C, Kroemer G. 2019. Methionine restriction for improving progeria: another autophagy-inducing anti-aging strategy? *Autophagy* 15:558–559.
- Barja G. 1998. Mitochondrial Free Radical Production and Aging in Mammals and Birds. *Ann. N. Y. Acad. Sci.* 854:224–238.
- Bozek K, Khrameeva EE, Reznick J, Omerbašić D, Bennett NC, Lewin GR, Azpurua J, Gorbunova V, Seluanov A, Regnard P, et al. 2017. Lipidome determinants of maximal lifespan in mammals. *Sci. Rep.* 7:1–5.
- Cabré R, Jové M, Naudí A, Ayala V, Piñol-Ripoll G, Gil-Villar MP, Dominguez-Gonzalez M, Obis È, Berdun R, Mota-Martorell N, et al. 2016. Specific Metabolomics Adaptations Define a Differential Regional Vulnerability in the Adult Human Cerebral Cortex. *Front. Mol. Neurosci.* 9:138.
- Caraveo G, Soste M, Cappelletti V, Fanning S, van Rossum DB, Whitesell L, Huang Y, Chung CY, Baru V, Zaichick S, et al. 2017. FKBP12 contributes to  $\alpha$ -synuclein toxicity by regulating the calcineurin-dependent phosphoproteome. *Proc. Natl. Acad. Sci.* 114:311–322.
- Caron A, Richard D, Laplante M. 2015. The Roles of mTOR Complexes in Lipid Metabolism. *Annu. Rev. Nutr.* 35:321–348.
- Chiang GG, Abraham RT. 2005. Phosphorylation of Mammalian Target of Rapamycin (mTOR) at Ser-2448 Is Mediated by p70S6 Kinase. *J. Biol. Chem.* 280:25485–25490.
- Cooper N, Thomas GH, FitzJohn RG. 2016. Shedding light on the ‘dark side’ of phylogenetic comparative methods. O’Hara RB, editor. *Methods Ecol. Evol.* 7:693–699.
- Cunningham JT, Rodgers JT, Arlow DH, Vazquez F, Mootha VK, Puigserver P. 2007. mTOR controls mitochondrial oxidative function through a YY1–PGC-1 $\alpha$  transcriptional complex. *Nature* 450:736–740.
- Düvel K, Yecies JL, Menon S, Raman P, Lipovsky AI, Souza AL, Triantafellow E, Ma Q, Gorski R, Cleaver S, et al. 2010. Activation of a Metabolic Gene Regulatory Network Downstream of mTOR Complex 1. *Mol. Cell* 39:171–183.
- Figueiredo VC, Markworth JF, Cameron-Smith D. 2017. Considerations on mTOR regulation at serine 2448: implications for muscle metabolism studies. *Cell. Mol. Life Sci.* 74:2537–2545.
- Fontana L, Partridge L, Longo VD. 2010. Extending Healthy Life Span--From Yeast to Humans. *Science* (80-. ). 328:321–326.
- Fredslund J, Schauer L, Madsen LH, Sandal N, Stougaard J. 2005. PriFi: using a multiple alignment of related sequences to find primers for amplification of homologs. *Nucleic Acids Res.* 33:516–520.
- Fushan AA, Turanov AA, Lee S-G, Kim EB, Lobanov A V., Yim SH, Buffenstein R, Lee S-R, Chang K-T, Rhee H, et al. 2015. Gene expression defines natural changes in mammalian lifespan. *Aging Cell* 14:352–365.

- Gu X, Orozco JM, Saxton RA, Condon KJ, Liu GY, Krawczyk PA, Scaria SM, Harper JW, Gygi SP, Sabatini DM. 2017. SAMTOR is an S-adenosylmethionine sensor for the mTORC1 pathway. *Science* (80-. ). 358:813–818.
- Hoeffler CA, Tang W, Wong H, Santillan A, Patterson RJ, Martinez LA, Tejada-Simon M V., Paylor R, Hamilton SL, Klann E. 2008. Removal of FKBP12 Enhances mTOR-Raptor Interactions, LTP, Memory, and Perseverative/Repetitive Behavior. *Neuron* 60:832–845.
- Jeon JS, Oh J-J, Kwak HC, Yun H, Kim HC, Kim Y-M, Oh SJ, Kim SK. 2018. Age-Related Changes in Sulfur Amino Acid Metabolism in Male C57BL/6 Mice. *Biomol. Ther. (Seoul)*. 26:167–174.
- Johnson SC, Rabinovitch PS, Kaeberlein M. 2013. mTOR is a key modulator of ageing and age-related disease. *Nature* 493:338–345.
- Jones OR, Scheuerlein A, Salguero-Gómez R, Camarda CG, Schaible R, Casper BB, Dahlgren JP, Ehrlén J, García MB, Menges ES, et al. 2014. Diversity of ageing across the tree of life. *Nature* 505:169–173.
- Jové M, Naudí A, Aledo JC, Cabré R, Ayala V, Portero-Otin M, Barja G, Pamplona R. 2013. Plasma long-chain free fatty acids predict mammalian longevity. *Sci. Rep.* 3:3346.
- Kapahi P, Chen D, Rogers AN, Katewa SD, Li PW-L, Thomas EL, Kockel L. 2010. With TOR, Less Is More: A Key Role for the Conserved Nutrient-Sensing TOR Pathway in Aging. *Cell Metab.* 11:453–465.
- Lewis KN, Rubinstein ND, Buffenstein R. 2018. A window into extreme longevity; the circulating metabolomic signature of the naked mole-rat, a mammal that shows negligible senescence. *GeroScience* 40:105–121.
- Liu Y, Song D, Xu B, Li H, Dai X, Chen B. 2017. Development of a matrix-based candidate reference material of total homocysteine in human serum. *Anal. Bioanal. Chem.* 409:3329–3335.
- Longo VD, Antebi A, Bartke A, Barzilai N, Brown-Borg HM, Caruso C, Curiel TJ, de Cabo R, Franceschi C, Gems D, et al. 2015. Interventions to Slow Aging in Humans: Are We Ready? *Aging Cell* 14:497–510.
- Lushchak O, Strilbytska O, Piskovatska V, Storey KB, Koliada A, Vaiserman A. 2017. The role of the TOR pathway in mediating the link between nutrition and longevity. *Mech. Ageing Dev.* 164:127–138.
- Ma S, Gladyshev VN. 2017. Molecular signatures of longevity: Insights from cross-species comparative studies. *Semin. Cell Dev. Biol.* 70:190–203.
- Ma S, Upneja A, Galecki A, Tsai Y-M, Burant CF, Raskind S, Zhang Q, Zhang ZD, Seluanov A, Gorbunova V, et al. 2016. Cell culture-based profiling across mammals reveals DNA repair and metabolism as determinants of species longevity. *Elife* 5:1–25.
- Ma S, Yim SH, Lee S-G, Kim EB, Lee S-R, Chang K-T, Buffenstein R, Lewis KN, Park TJ, Miller RA, et al. 2015. Organization of the Mammalian Metabolome according to Organ Function, Lineage Specialization, and Longevity. *Cell Metab.* 22:332–343.
- Martínez-Cisuelo V, Gómez J, García-Junceda I, Naudí A, Cabré R, Mota-Martorell N, López-Torres M, González-Sánchez M, Pamplona R, Barja G. 2016. Rapamycin reverses age-related increases in mitochondrial ROS production at complex I, oxidative stress,

- accumulation of mtDNA fragments inside nuclear DNA, and lipofuscin level, and increases autophagy, in the liver of middle-aged mice. *Exp. Gerontol.* 83:130–138.
- Mota-Martorell N, Pradas I, Jové M, Naudí A, Pamplona R. 2019. Biosíntesis de novo de glicerofosfolípidos y longevidad. *Rev. Esp. Geriatr. Gerontol.* 54:88–93.
- Muntané G, Farré X, Rodríguez JA, Pegueroles C, Hughes DA, de Magalhães JP, Gabaldón T, Navarro A. 2018. Biological Processes Modulating Longevity across Primates: A Phylogenetic Genome-Phenome Analysis. Wray G, editor. *Mol. Biol. Evol.* 35:1990–2004.
- Nascimento EBM, Snel M, Guigas B, van der Zon GCM, Kriek J, Maassen JA, Jazet IM, Diamant M, Ouwens DM. 2010. Phosphorylation of PRAS40 on Thr246 by PKB/AKT facilitates efficient phosphorylation of Ser183 by mTORC1. *Cell. Signal.* 22:961–967.
- Naudí A, Jové M, Ayala V, Portero-Otín M, Barja G, Pamplona R. 2013. Membrane lipid unsaturation as physiological adaptation to animal longevity. *Front. Physiol.* 4:372.
- Pamplona R, Barja G. 2006. Mitochondrial oxidative stress, aging and caloric restriction: The protein and methionine connection. *Biochim. Biophys. Acta - Bioenerg.* 1757:496–508.
- Pamplona R, Barja G. 2007. Highly resistant macromolecular components and low rate of generation of endogenous damage: Two key traits of longevity. *Ageing Res. Rev.* 6:189–210.
- Pamplona R, Barja G. 2011. An evolutionary comparative scan for longevity-related oxidative stress resistance mechanisms in homeotherms. *Biogerontology* 12:409–435.
- Pamplona R, Barja G, Portero-Otín M. 2002. Membrane Fatty Acid Unsaturation, Protection against Oxidative Stress, and Maximum Life Span. *Ann. N. Y. Acad. Sci.* 959:475–490.
- Papadopoli D, Boulay K, Kazak L, Pollak M, Mallette F, Topisirovic I, Hulea L. 2019. mTOR as a central regulator of lifespan and aging. *F1000Research* 8:998.
- Passtoors WM, Beekman M, Deelen J, van der Breggen R, Maier AB, Guigas B, Derhovanessian E, van Heemst D, de Craen AJM, Gunn DA, et al. 2013. Gene expression analysis of mTOR pathway: association with human longevity. *Aging Cell* 12:24–31.
- Perez-Campo R, López-Torres M, Cadenas S, Rojas C, Barja G. 1998. The rate of free radical production as a determinant of the rate of aging: evidence from the comparative approach. *J. Comp. Physiol. B Biochem. Syst. Environ. Physiol.* 168:149–158.
- Ruckenstuhl C, Netzberger C, Entfellner I, Carmona-Gutierrez D, Kickenweiz T, Stekovic S, Gleixner C, Schmid C, Klug L, Sorgo AG, et al. 2014. Lifespan Extension by Methionine Restriction Requires Autophagy-Dependent Vacuolar Acidification. Kim SK, editor. *PLoS Genet.* 10:e1004347.
- Sahm A, Bens M, Henning Y, Vole C, Groth M, Schwab M, Hoffmann S, Platzer M, Szafranski K, Dammann P. 2018. Higher gene expression stability during aging in long-lived giant mole-rats than in short-lived rats. *Aging (Albany, NY)*. 10:3938–3956.
- Schieke SM, Phillips D, McCoy JP, Aponte AM, Shen R-F, Balaban RS, Finkel T. 2006. The Mammalian Target of Rapamycin (mTOR) Pathway Regulates Mitochondrial Oxygen Consumption and Oxidative Capacity. *J. Biol. Chem.* 281:27643–27652.
- Schwanhäusser B, Busse D, Li N, Dittmar G, Schuchhardt J, Wolf J, Chen W, Selbach M. 2011.

- Global quantification of mammalian gene expression control. *Nature* 473:337–342.
- Selman C, Tullet JMA, Wieser D, Irvine E, Lingard SJ, Choudhury AI, Claret M, Al-Qassab H, Carmignac D, Ramadani F, et al. 2009. Ribosomal Protein S6 Kinase 1 Signaling Regulates Mammalian Life Span. *Science* (80- ). 326:140–144.
- Simonsen A, Cumming RC, Brech A, Isakson P, Schubert DR, Finley KD. 2008. Promoting basal levels of autophagy in the nervous system enhances longevity and oxidant resistance in adult *Drosophila*. *Autophagy* 4:176–184.
- Singh PP, Demmitt BA, Nath RD, Brunet A. 2019. The Genetics of Aging: A Vertebrate Perspective. *Cell* 177:200–220.
- Tyshkovskiy A, Bozaykut P, Borodinova AA, Gerashchenko M V., Ables GP, Garratt M, Khaitovich P, Clish CB, Miller RA, Gladyshev VN. 2019. Identification and Application of Gene Expression Signatures Associated with Lifespan Extension. *Cell Metab.* 30:573-593.e8.
- Valvezan AJ, Manning BD. 2019. Molecular logic of mTORC1 signalling as a metabolic rheostat. *Nat. Metab.* 1:321–333.
- Weichhart T. 2018. mTOR as Regulator of Lifespan, Aging, and Cellular Senescence: A Mini-Review. *Gerontology* 64:127–134.
- Wu JJ, Liu J, Chen EB, Wang JJ, Cao L, Narayan N, Fergusson MM, Rovira II, Allen M, Springer DA, et al. 2013. Increased Mammalian Lifespan and a Segmental and Tissue-Specific Slowing of Aging after Genetic Reduction of mTOR Expression. *Cell Rep.* 4:913–920.

Figure 1

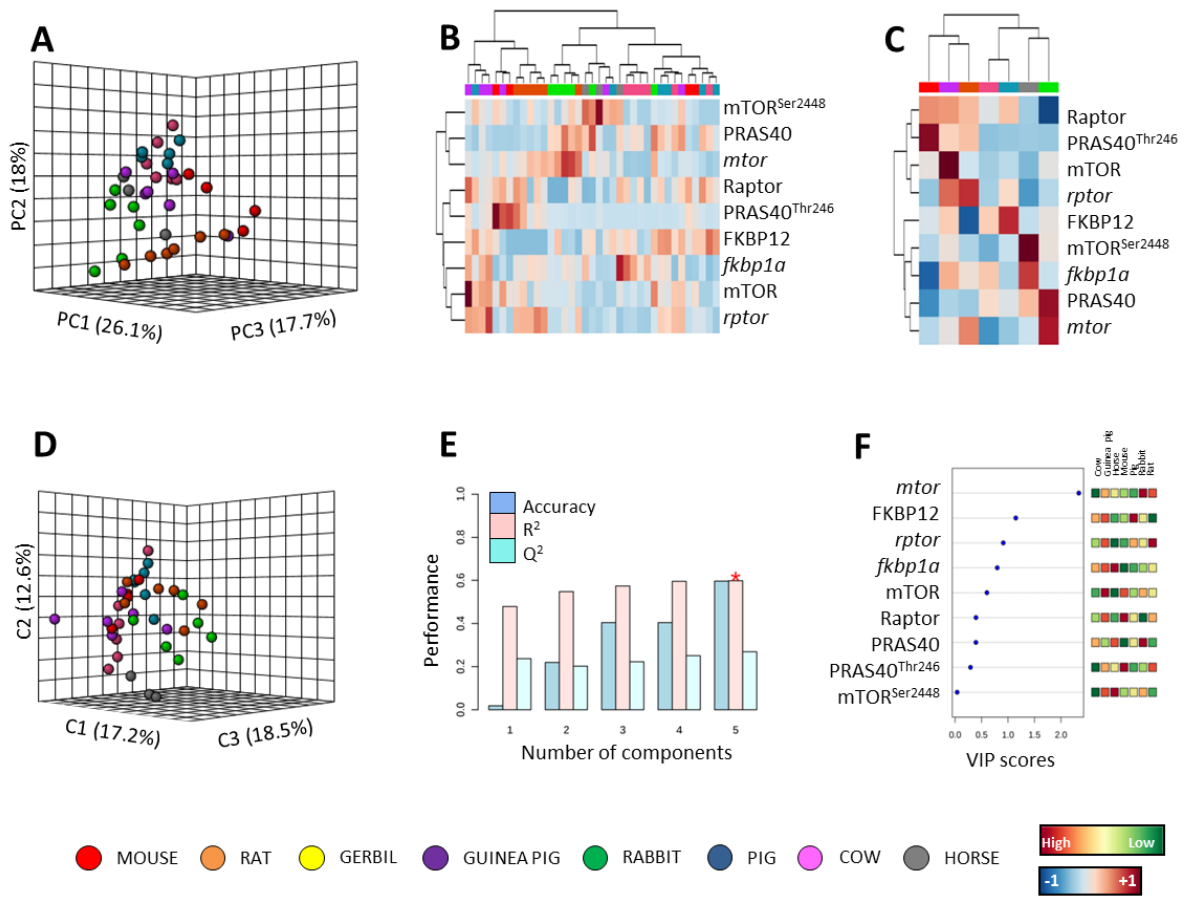


Figure 2

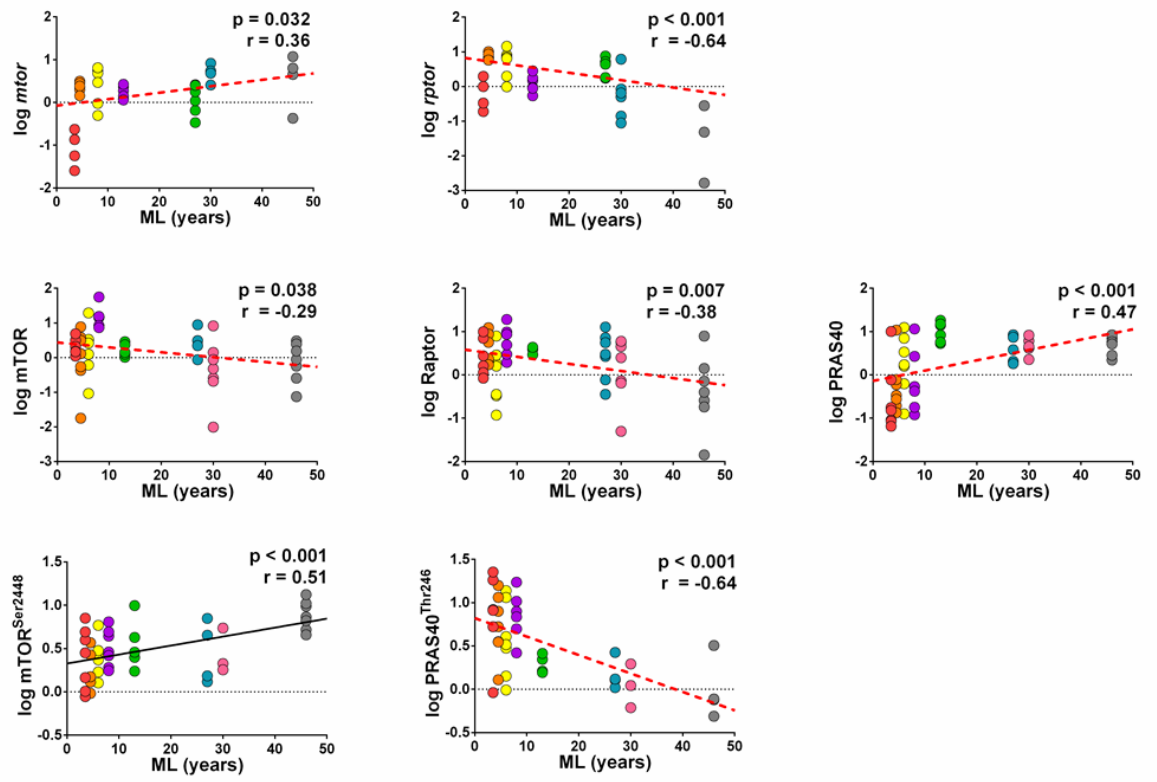


Figure 3

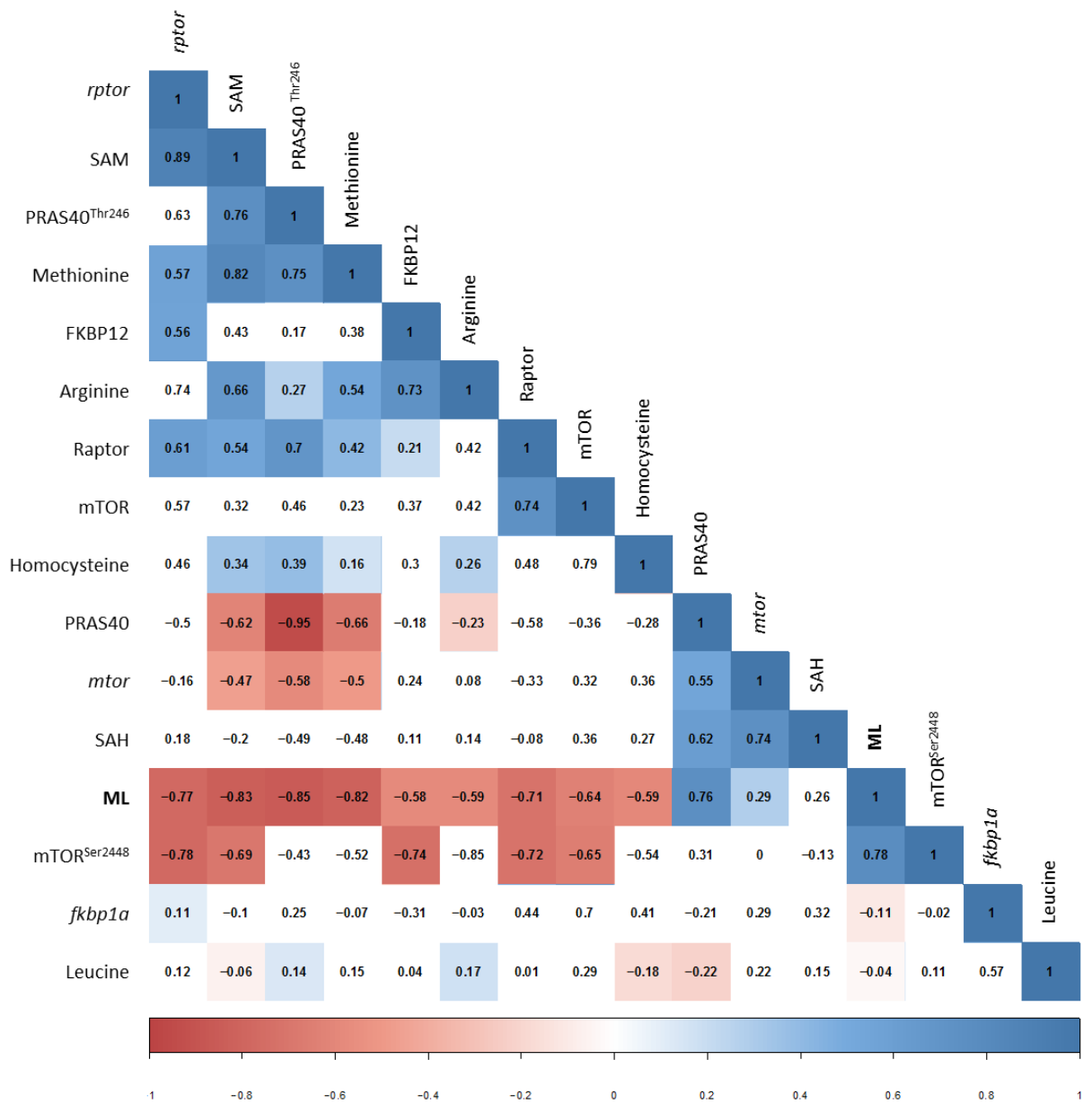


Figure 4

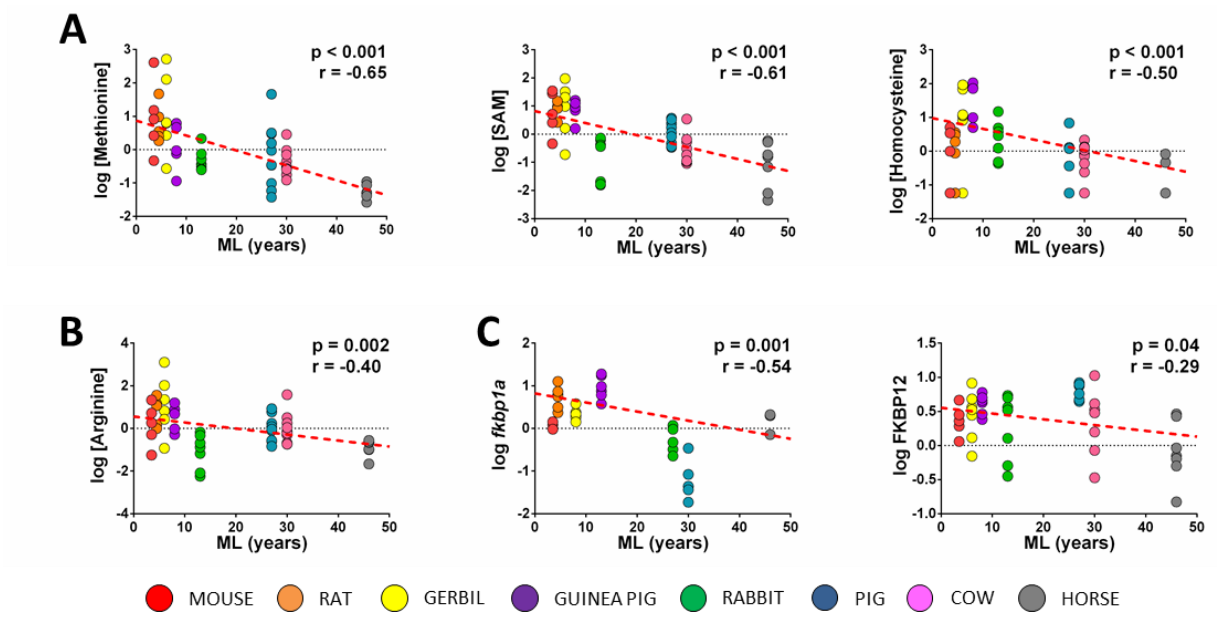


Figure 5

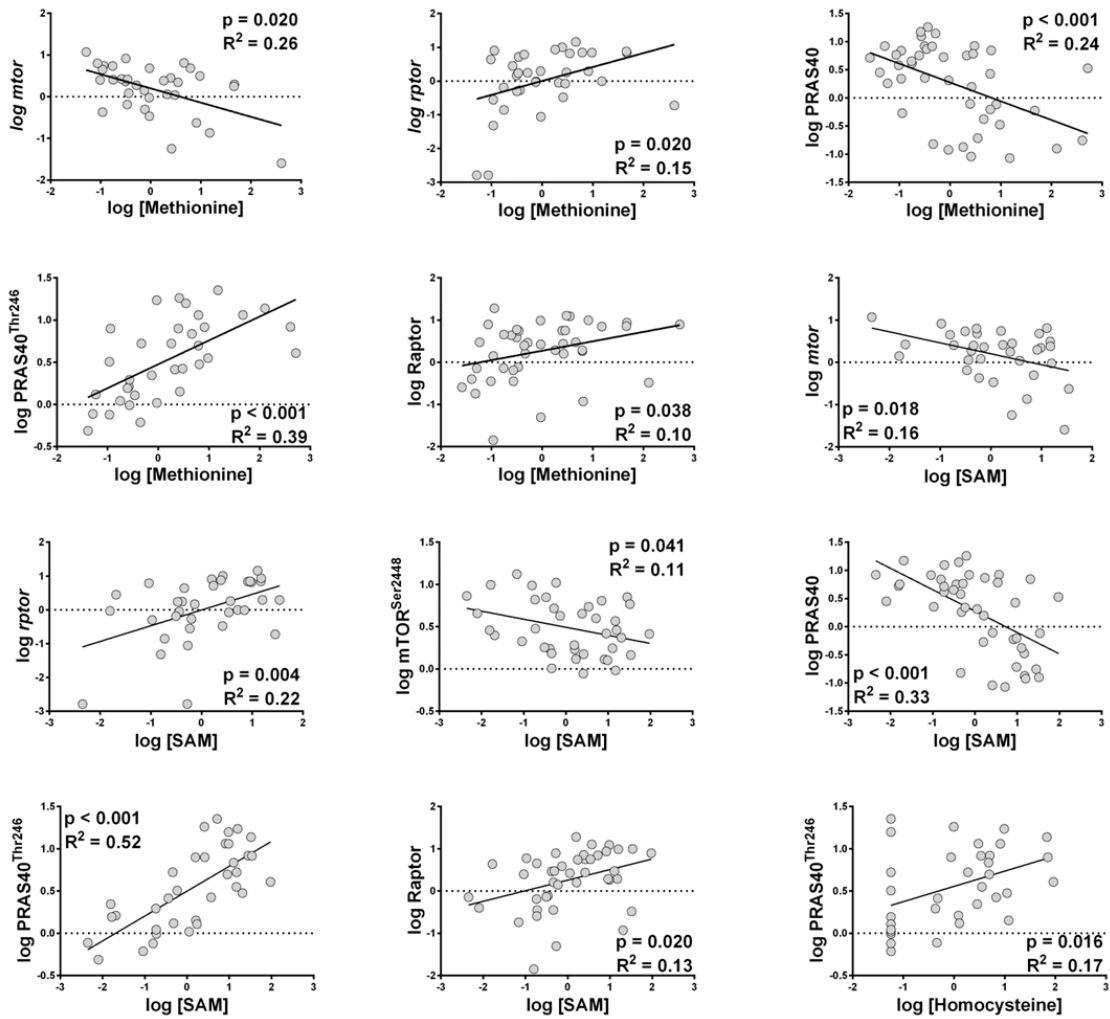


Figure 6

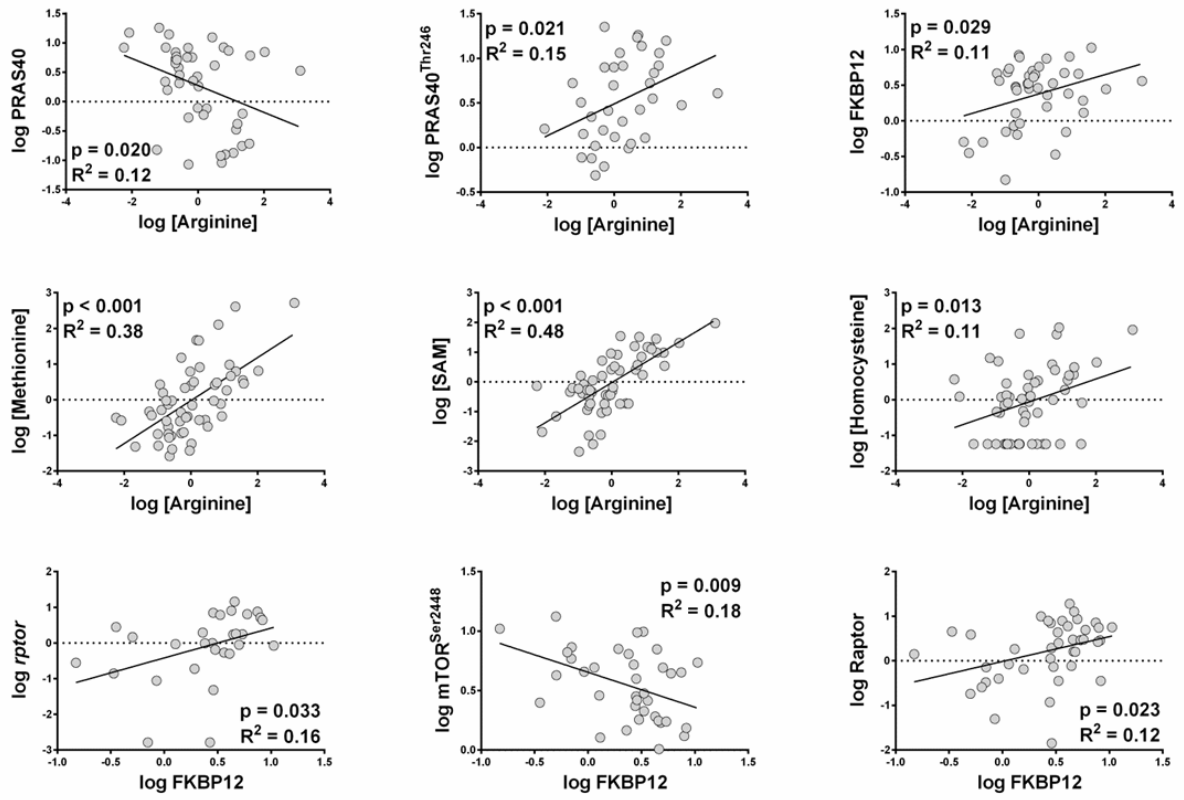


Figure 7

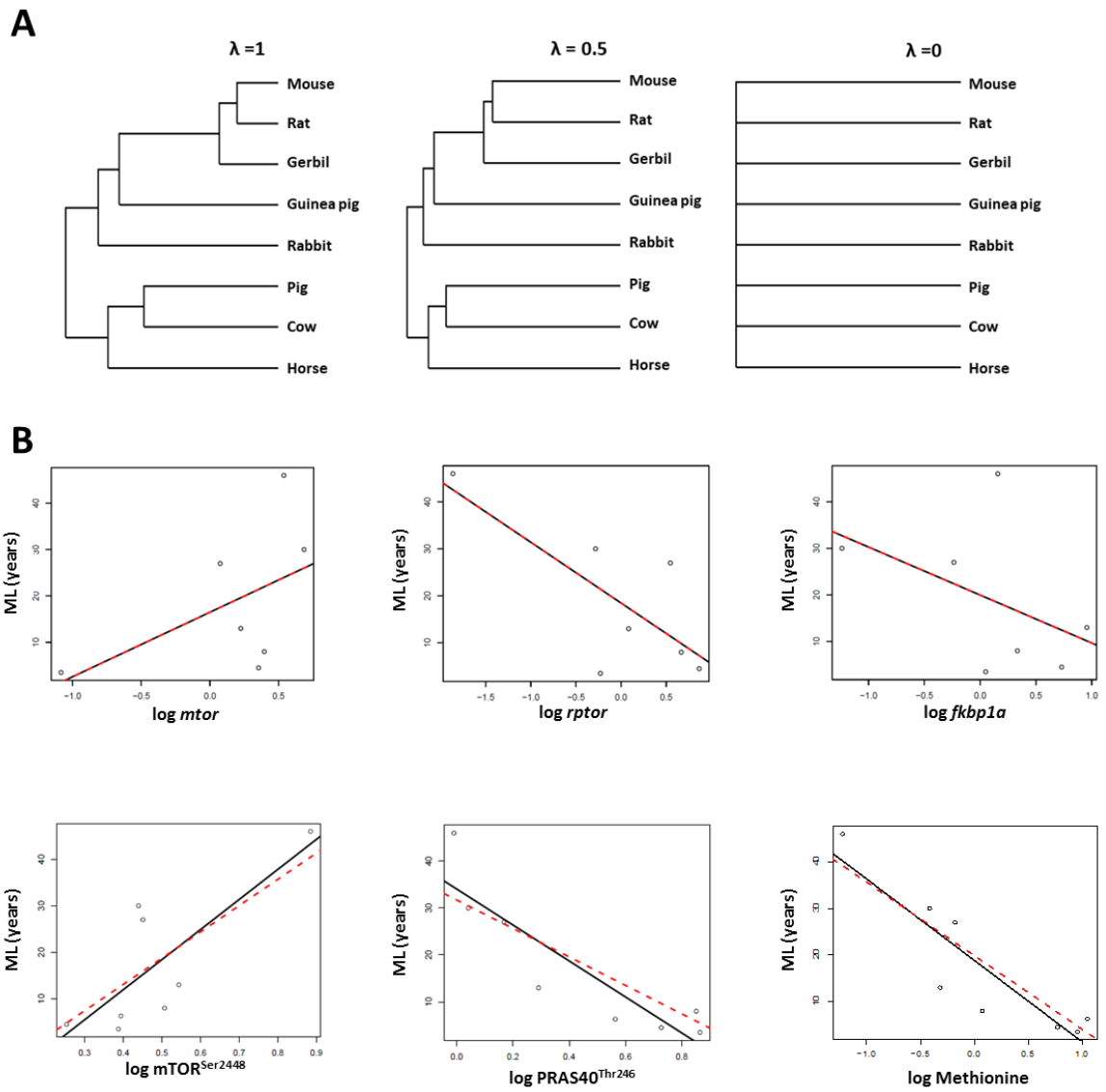
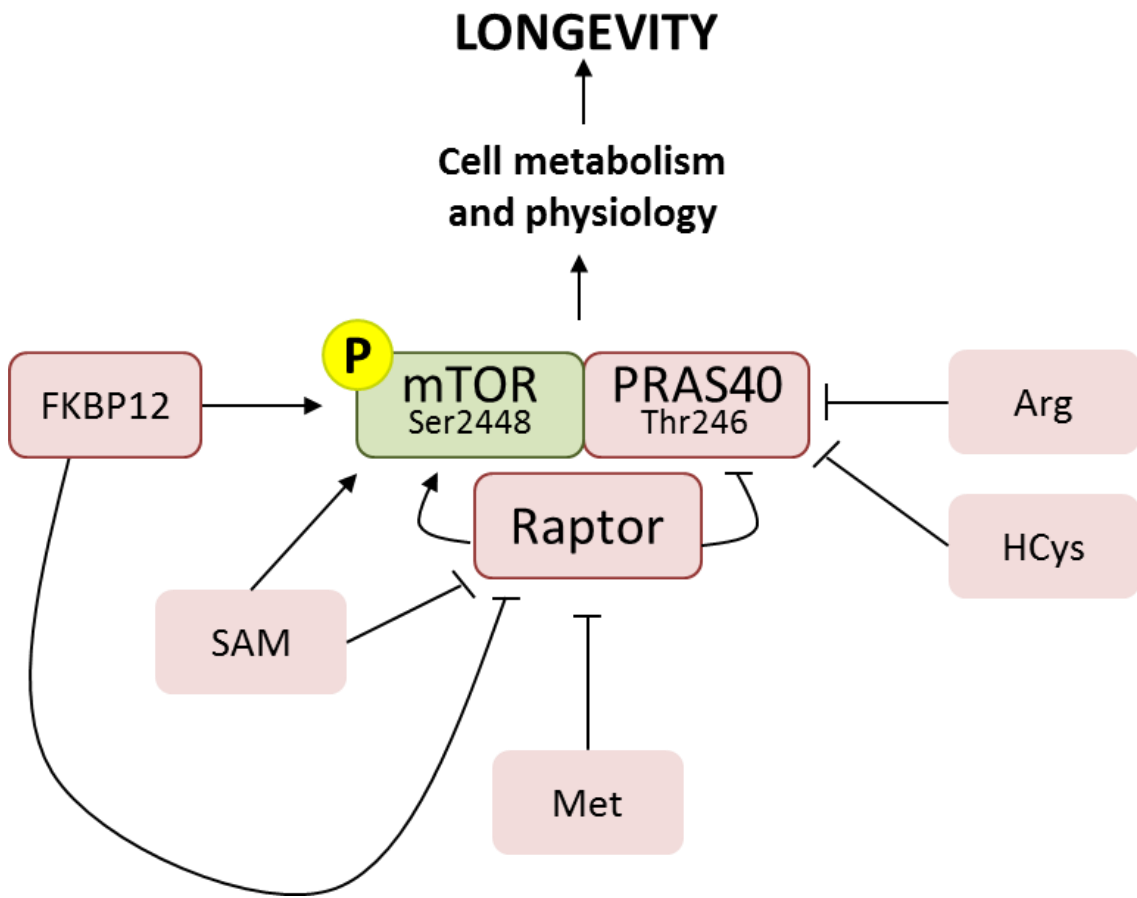
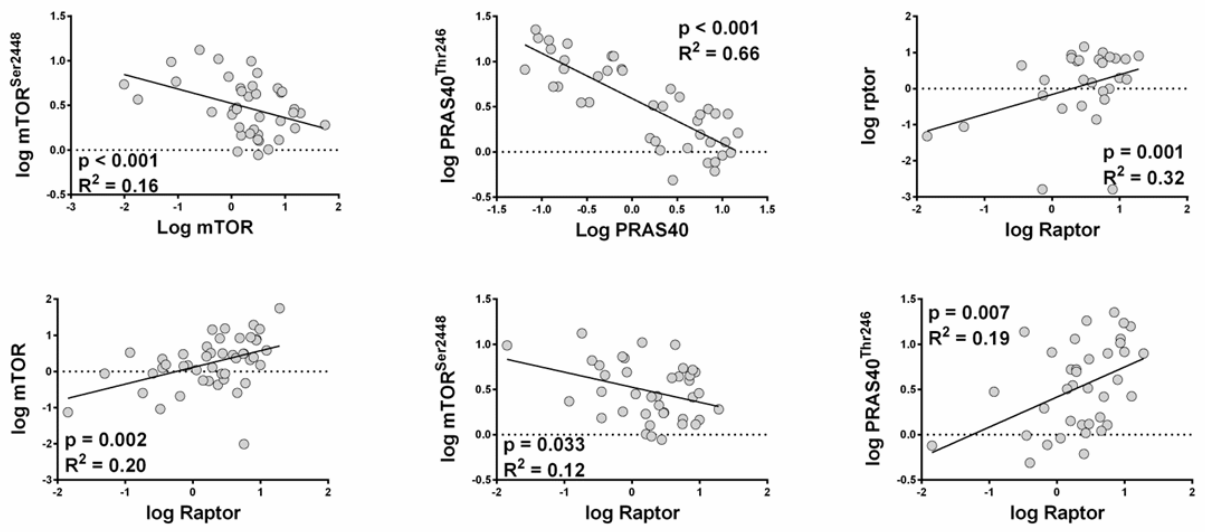


Figure 8



## Supplementary Figure 1



Supplementary Figure 2

